An essential GDP-Fuc: β-D-Gal α-1,2-fucosyltransferase is located in the mitochondrion of Trypanosoma brucei — Source link ↗

Giulia Bandini, Sebastian Damerow, Maria Lucia S. Güther, Angela Mehlert ...+3 more authors

Institutions: University of Dundee, Washington University in St. Louis

Topics: Fucosyltransferase, Fucosylation, Trypanosoma brucei, Fucose and Glycan

Related papers:

- An essential, kinetoplastid-specific GDP-Fuc: β-D-Gal α-1,2-fucosyltransferase is located in the mitochondrion of Trypanosoma brucei.

- The de novo synthesis of GDP-fucose is essential for flagellar adhesion and cell growth in Trypanosoma brucei.

- A broadly active fucosyltransferase LmjFUT1 whose mitochondrial localization and activity are essential in parasitic Leishmania.

- A broadly active fucosyltransferase LmjFUT1 whose mitochondrial localization and catalytic activity is essential in parasitic Leishmania major

- Trypanosoma brucei UDP-glucose:glycoprotein glucosyltransferase has unusual substrate specificity and protects the parasite from stress.

Share this paper: 🟦 🐦 in ✉

1   **An essential GDP-Fuc: β-*D*-Gal α-1,2-fucosyltransferase is located in the mitochondrion of**

2   ***Trypanosoma brucei***

3   Giulia Bandini[a,1,2], Sebastian Damerow[a,1,3], Maria Lucia Sampaio Güther[a], Angela Mehlert[a],

4   Hongjie Guo[b], Stephen M. Beverley[b] and Michael A. J. Ferguson[a,4]

5

6   [a]Wellcome Centre for Anti-Infectives Research, School of Life Sciences, University of Dundee,

7   Dundee, DD1 5EH, United Kingdom.

8   [b]Department of Molecular Microbiology, Washington University School of Medicine, St. Louis,

9   MO 63110, USA.

10   [1]These authors contributed equally to this work.

11   [2]Current address: Department of Molecular and Cell Biology, Boston University Goldman School

12   of Dental Medicine, Boston MA 02118, USA

13   [3]Current address: Richter-Helm BioLogics GmbH, Suhrenkamp 59, 22335 Hamburg, Germany

14

15   [4]Corresponding author. Mailing address: Wellcome Centre for Anti-Infectives Research, School

16   of Life Sciences, University of Dundee, Dow St., Dundee DD1 5EH, Scotland, United Kingdom.

17   Phone: 44-1382-384219. Fax: 44-1382-348896. E-mail: m.a.j.ferguson@dundee.ac.uk

18

25

ABSTRACT

The biosynthesis of guanosine 5′-diphospho-β-L-fucose (GDP-Fuc), the activated donor for fucose, has been shown to be essential in the parasite *Trypanosoma brucei*. Fucose is a common constituent of eukaryotic glycan structures, but it has been rarely found in trypanosomatid glycoconjugates. A single putative *T. brucei* fucosyltransferase (*TbFUT1*) gene was identified in the trypanosome genome. The encoded TbFUT1 protein was enzymatically active when expressed in *Escherichia coli*. Structural characterization of its reaction products identified it as a GDP-Fuc: β-D-galactose α-1,2-fucosyltransferase, with a preference for a Galβ1,3GlcNAcβ1-O-R acceptor motif among the substrates tested. Conditional null mutants of the *TbFUT1* gene demonstrated that it is essential for growth of the mammalian-infective bloodstream form and insect vector dwelling procyclic form of the parasite. Unexpectedly, TbFUT1 was localized in the mitochondrion of *T. brucei* and found to be essential for mitochondrial function in bloodstream form trypanosomes, suggesting this kinetoplastid parasite possesses an unprecedented and essential mitochondrial fucosyltransferase activity.

41 **SIGNIFICANCE**

42 The sugar fucose is a well-known component of cell-surface glycoproteins and glycolipids and

43 typically plays roles in cell-cell adhesion. Fucose is generally incorporated into glycoproteins and

44 glycolipids by fucosyltransferase enzymes that reside in the Golgi apparatus. Here we show that

45 the single fucosyltransferase of the protozoan parasite *Trypanosoma brucei*, causative agent of

46 human and animal African trypanosomiasis, resides in the mitochondrion and not the Golgi

47 apparatus. While the exact role of fucosylation in the parasite mitochondrion remains to be

48 determined, it is essential for mitochondrial function and for parasite growth and survival. The

49 unusual nature of this parasite enzyme, and its orthologues in related parasite pathogens, suggests

50 that selective inhibitors may have therapeutic potential across a family of parasites.

51

INTRODUCTION

The protozoan parasites of the *Trypanosoma brucei* group are the causative agents of human and animal African trypanosomiasis. Bloodstream form *T. brucei* are ingested by the tsetse fly vector and differentiates into the procyclic form parasites to colonize the tsetse midgut. To infect a new mammalian host, *T. brucei* undergoes a series of differentiations that allows it to colonize the salivary gland of the fly and to be transferred to a new host during a subsequent blood meal (1).

The surface coat of the bloodstream form is characterized by the GPI-anchored*, N*-glycosylated variant surface glycoprotein (VSG) (2–5), while procyclic cells express a family of GPI-anchored proteins called procyclins (6–9), free glycoinositolphospholipids (10–12) and a high molecular weight glycoconjugate complex (13). The importance of glycoproteins to parasite survival and infectivity has led to the investigation of enzymes of GPI anchor (14–17) and nucleotide sugar (18–24) biosynthesis as potential therapeutic targets.

Nucleotide sugars are used as glycosyl donors in many glycosylation reactions. GDP-Fucose (GDP-Fuc) was identified in the nucleotide sugar pools of *T. brucei*, *Trypanosoma cruzi* and *Leishmania major* (25) and its biosynthesis is essential for parasite growth in procyclic and bloodstream form *T. brucei* (26) and in *L. major* promastigotes (27). Interestingly, *T. brucei* and *L. major* use different pathways to synthesize GDP-Fuc. *T. brucei* utilizes the *de novo* pathway in which GDP-Fuc is synthesised from GDP-Mannose via GDP-mannose-4,6-dehydratase (GMD) and GDP-4-keto-6-deoxy-D-mannose epimerase/reductase (GMER) (25, 26). Conversely, *L. major* has two related bifunctional arabino/fuco-kinase/pyrophosphorylases, AFKP80 and FKP40 that synthesise GDP-Fuc from free fucose (27). The only structurally-defined fucose-containing oligosaccharide in trypanosomatids is the low-abundance Ser/Thr-phosphodiester-linked glycan on *T. cruzi* gp72, a glycoprotein that has been implicated in flagellar attachment (28–30).

76   Fucosyltransferases (FUTs) catalyse the transfer of fucose from GDP-Fuc to glycan and

77   protein acceptors and are classified into two superfamilies (31, 32). One superfamily contains all

78   α1,3/α1,4-FUTs (Carbohydrate Active EnZyme, CAZy, family GT10) and the other contains all

79   α1,2-, α1,6- and protein *O*-fucosyltransferases (GT11, GT23, GT37, GT65 and GT68) (33). In

80   eukaryotes, the vast majority of fucosyltransferases are type II transmembrane Golgi proteins

81   (34), but two exceptions have been described: (i) PgtA, a cytoplasmic bifunctional β1,3-

82   galactosyltransferase / α1,2-FUT found in *Dictyostelium discoideum* and *Toxoplasma gondii* (35,

83   36) that is part of an oxygen-sensitive glycosylation pathway that attaches a pentasaccharide to

84   the Skp1-containing ubiquitin ligase complex (37); and (ii) SPINDLY, a protein *O*-

85   fucosyltransferase that modifies nuclear proteins in *Arabidopsis thaliana* and *T. gondii* (38, 39).

86   Unusually, *T. brucei* and other kinetoplastids contain a single mitochondrion. In the

87   bloodstream form of the parasite this organelle has a tubular structure, while in the procyclic form

88   it is organized in a complex network with numerous cristae, reflecting the absence and presence,

89   respectively, of oxidative phosphorylation (1, 40). The parasite mitochondrion is further

90   characterized by a disc-shaped DNA network called the kinetoplast (41) that is physically linked

91   with the flagellum basal body (42, 43).

92   While secretory pathway and nuclear/cytosolic glycosylation systems have been studied

93   extensively, little is known about glycosylation within mitochondria. A glycoproteomic approach

94   in yeast revealed several mitochondrial glycoproteins (44), but it was not determined whether

95   these were imported from secretory pathway or glycosylated within the mitochondria by as yet

96   unknown glycosyltransferases. The only characterized example of a mitochondrial

97   glycosyltransferase is the mitochondrial isoform of mammalian *O*-GlcNAc transferase (OGT). *O*-

98   GlcNAcylation is a cycling modification, involved in signalling, in which OGT adds GlcNAc to

99   Ser/Thr residues and *O*-GlcNAcase (OGA) removes it (45). Recent studies have shown that both

5

100   mitochondrial OGT (mOGT) and OGA are present and active in mammalian mitochondria and

101   putative mitochondrial targets have been identified (46, 47). Further, a mammalian mitochondrial

102   UDP-GlcNAc transporter associated with mitochondrial *O*-GlcNAcylation has been recently

103   described (46). However, orthologues of OGT and OGA genes are not present in kinetoplastids.

104   Here, we report on a gene (*TbFUT1*) encoding a mitochondrial α-1,2-fucosyltransferase

105   protein (TbFUT1) in *T. brucei* that is essential to parasite survival.

106

107   **RESULTS**

108   ***Identification, cloning and sequence analysis of TbFUT1.*** The CAZy database lists eight

109   distinct FUT families: GT10, 11, 23, 37, 56, 65, 68 and 74 (32). One or more sequences from

110   each family were selected for BLASTp searches of the predicted proteins from the *T. brucei, T.*

111   *cruzi* and *L. major* genomes (Table S1). Strikingly, only one putative *T. brucei* fucosyltransferase

112   gene (*TbFUT1*) was identified from the *T. brucei* genome (GeneDB ID: Tb927.9.3600) belonging

113   to the GT11 family, which is comprised almost exclusively of α-1,2-FUTs (31, 48). Homologues

114   of *TbFUT1* were also found in the *T. cruzi* and *L. major* genomes and, unlike *T. brucei*, *T. cruzi*

115   and *L. major* also encode for GT10 FUT genes (Table S1).

116   The TbFUT1 predicted amino acid sequence shows relatively low sequence identity to

117   previously characterized GT11 FUTs, for example to *H. pylori* (26%) or human FUT2 (21%) (49,

118   50). Nevertheless, conserved motifs characteristic of this family can be clearly identified (Fig.

119   S1*A*) (33, 51). Motif I (aa 153-159) is shared with α-1,6-FUTs and has been implicated in the

120   binding of GDP-Fuc (52), whereas no clear functions have yet been assigned to motifs II, III and

121   IV (aa 197-207, 265-273 and 13-18, respectively). Although TbFUT contains a possible

122   transmembrane (TM) domain at its N-terminus, as would be expected of a typical Golgi-localized

123   fucosyltransferase (34), this putative TM domain (residues 6-28) overlaps with the

6

124   fucosyltransferase motif IV, which normally occurs after the TM domain (Fig. S1*A*). Indeed,

125   further analysis of the TbFUT predicted amino acid sequence using *PSort II (53), Target P* (54)

126   and *Mitoprot* (55) suggested mitochondrial localization and identified a putative mitochondrial

127   targeting motif (M/L..RR) with RR at sequence position +30, similar to those described for other

128   eukaryotes. Conservation of this targeting motif has been previously shown for other parasite

129   mitochondrial proteins (56, 57). Further BLASTp searches show that there is generally a single

130   TbFUT1 gene homologue in each kinetoplastid species, and a phylogram of FUT sequences

131   shows that TbFUT1 homologues form a distinct clade closest to bacterial α-1,2-

132   fucosyltransferases (Fig. S1*B*).

133

134   ***Recombinant expression of TbFUT1***. The *TbFUT1* ORF was amplified from *T. brucei* 427

135   genomic DNA and cloned in the pGEX6P1 expression vector. The resulting construct

136   (pGEX6P1-GST-PP-*TbFUT1*) encoded for the *TbFUT1* ORF with a glutathione-S-transferase

137   (GST) tag at its N-terminus and a PreScission™ Protease (PP) cleavage site between the two

138   protein-encoding sequences. Sequencing identified a few nucleotide and amino acid differences

139   between the 427 and 927 strains, all of which are consistent with the partial genome assembly of

140   strain 427 (58). The pGEX6P1-GST-PP-*TbFUT1* construct was expressed in *E. coli* and the

141   fusion protein purified as described in Methods and Methods SI. The identities of the two higher

142   molecular weight bands (Fig. S2, lane 8) were determined by peptide mass fingerprinting. The

143   most abundant band was identified as TbFUT1, while the fainter band was identified as a subunit

144   of the *E. coli* GroEL chaperonin complex. The apparent molecular weight of GST-PP-TbFUT1

145   chimeric protein (57 kDa) was consistent with the predicted theoretical molecular weight (58.1

146   kDa).

147

7

148 ***Recombinant TbFUT1 is active in vitro.*** The recombinantly expressed GST-TbFUT1 fusion

149 protein was tested for activity by incubation with GDP-[^{3}H]Fuc as a donor and a panel of

150 commercially available mono- to octasaccharides (Table 1) selected from the literature as

151 possible α-1,2-FUT substrates (48, 49, 51). The effectiveness of each acceptor was evaluated

152 based on the presence/absence and intensities of the TLC bands corresponding to the

153 radiolabelled reaction products (Fig. 1 and Table 1). GST-TbFUT1 showed its best activity with

154 Galβ1,3GlcNAc (LNB) (Fig. 1, lane 2 and 5) and its β-O-Methyl glycoside (Fig. 1, lane 23).

155 Other larger oligosaccharides containing Galβ1,3GlcNAcβ1-O-R as a terminal motif (LNT and

156 LNH) were also good acceptors (Fig. 1, lanes 13 and 16), with the exception of iLNO (Fig. 1,

157 lane 15). Lactose was also an acceptor (Fig. 1, lane 1), while LacNAc and the LacNAc-

158 terminating branched hexasaccharide LNnH were weak acceptors (Fig. 1, lanes 3 and 12).

159 Interestingly, TbFUT1 was also able to transfer fucose to 3'-fucosyllactose, albeit inefficiently

160 (Fig. 1, lane 18), whereas no transfer could be seen to Galβ1,6GlcNAc (Fig. 1, lane 17) or to free

161 Gal or β-Gal-O-methyl (Fig. 1, lanes 11 and 22). As expected, no products were observed when

162 acceptor oligosaccharides were omitted from the reaction (Fig. 1, lane 6). To confirm the detected

163 activities were specific to the recombinant GST-TbFUT1, and not due to some co-purifying

164 endogenous *E. coli* contaminant, the assay was also performed using material prepared from *E.*

165 *coli* expressing the empty pGEX6P1 vector. No transfer of radiolabelled fucose could be

166 observed in these cases (Fig. 1, lanes 7-9).

167 A band with the same mobility as free fucose was always present in the assay reactions

168 and was considerably stronger in the presence of the GST-TbFUT1 preparation (Fig. 1, lanes 1-6

169 and 11-24), than when GDP-[^{3}H]Fuc was incubated with the reaction buffer alone (Fig. 1, lane

170 10) or in the presence of the material purified from the *E. coli* cells transformed with the empty

171 vector (Fig. 1, lanes 7-9). These data suggest that TbFUT1 has a significant propensity to transfer

8

172   Fuc to water. Interestingly, one of the substrates (LNB-O-Me; Galβ1,3GlcNAcβ1-O-methyl)

173   suppressed the amount of free Fuc produced in the reaction (Fig. 1, lane 23), suggesting that this

174   sugar may bind more tightly to the TbFUT1 acceptor site than the other glycans and thus prevent

175   the transfer of Fuc from GDP-Fuc to water.

176   The inverting α-1,2 and α-1,6-FUTs are independent of divalent cations for their activity

177   (51, 59–61). To study the dependence of TbFUT1 on these co-factors, the assay was repeated in

178   buffer without divalent cations or containing EDTA. No change in activity was observed in either

179   case, indicating TbFUT1 does not require divalent cations for its activity (Fig. S3).

180

181   ***Characterization of the TbFUT1 reaction product.*** The glycan reaction products were

182   structurally characterized to determine the anomeric and stereochemical specificity of TbFUT1.

183   Initially, we performed exoglycosidase and/or acid treatment of the radiolabelled reaction

184   products (recovered by preparative TLC) utilizing Lac, LacNAc and LNB as substrates. The

185   tritium label ran with the same mobility as authentic Fuc after acid hydrolysis of all three

186   products (Fig. S4*A* and *C*) and after *Xanthomonas manihotis* α-1,2-fucosidase digestion of the

187   Lac and LNB products (Fig. S4*B* and *C*). These data suggest that [^{3}H]Fuc was transferred in α1,2

188   linkage to the acceptor disaccharides.

189   To obtain additional and definitive data, we performed a large-scale activity assay using

190   LNB-O-Me as an acceptor and purified the reaction product by normal phase HPLC. Fractions

191   containing the putative fucosylated trisaccharide product (Fig. S5) were pooled and analysed for

192   their neutral monosaccharide content, which showed the presence of Fuc, Gal and GlcNAc. The

193   purified reaction product was then permethylated and analysed by ESI-MS (Fig. 2*A*), which

194   confirmed that the main product was a trisaccharide of composition $dHex_1Hex_1HexNAc_1$. The

195   MS/MS spectrum was also consistent with the dHex residue being attached to the Hex, rather

9

196   than HexNAc, residue (Fig. 2*B*). Subsequently, partially methylated alditol acetates (PMAAs)

197   were generated from the purified trisaccharide product and analysed by GC-MS. This analysis

198   identified derivatives consistent with the presence of non-reducing terminal-Fuc, 2-*O*-substituted

199   Gal and 3-*O*-substituted GlcNAc (Fig. S6 and Table 2), consistent with Fuc being linked to the

200   position 2 of Gal. The GC-MS methylation linkage analysis also revealed a trace of 2-*O*-

201   substituted Fuc in the sample which, together with the observation that 3'-FL can act as a weak

202   substrate (Fig. 1, lane 18 and Table 1), may suggest that TbFUT1 can also form Fucα1,2Fuc

203   linkages.

204   The purified TbFUT1 reaction product was also exchanged into deuterated water (^2H_2O)

205   and analysed by one-dimensional ^{1}H-NMR and two-dimensional ^{1}H-ROESY (Rotating frame

206   Overhouser Effect SpectroscopY). The ^{1}H-NMR spectrum showed a doublet at about 5.1 ppm,

207   consistent with the signal from the proton on the anomeric carbon (H_1) of an α-Fuc residue (Fig.

208   3*A*). A characteristic doublet for the anomeric proton of a β-Gal residue was also observed at 4.5

209   ppm. In the ^{1}H-ROESY spectrum, a cross-peak (labelled *a*) could be observed indicating a

210   through-space connectivity between the H_1 of α-Fuc and the H_2 of a β-Gal, consistent with a

211   Fucα1,2Gal linkage in the TbFUT1 reaction product (Fig. 3*B*). The chemical shifts that could be

212   clearly assigned by either one-dimensional ^{1}H-NMR or two-dimensional ^{1}H-ROESY are listed in

213   (Table 3).

214   Taken together, these data unambiguously define the structure of the TbFUT1 reaction

215   product with GDP-Fuc and LNB-O-Me as Fucα1,2Galβ1,3GlcNAcβ1-O-CH$_3$ which, in turn,

216   defines TbFUT1 as having a GDP-Fuc : βGal α-1,2 fucosyltransferase activity with a preference

217   for a Galβ1,3GlcNAcβ1-O-R acceptor motif.

218

219   ***Generation of TbFUT1 conditional null mutants in procyclic and bloodstream form T. brucei.***

220   Semi-quantitative RT-PCR showed that *TbFUT1* mRNA was present in both bloodstream form

221   and procyclic form *T. brucei*. We therefore sought to explore TbFUT1 function in both lifecycle

222   stages by creating *TbFUT1* conditional null mutants. The strategies used to generate the mutants

223   are described in (Fig. 4). The creation of these mutants was possible because genome assembly

224   indicated *TbFUT1* to be present as a single copy per haploid genome, and Southern blot analysis

225   using a *TbFUT1* probe was consistent with this prediction (Fig. S7). In procyclic cells (Fig. 4, left

226   panel), the first *TbFUT1* allele was replaced by homologous recombination with linear DNA

227   containing the puromycin resistance gene (*PAC*) flanked by about 500 bp of the *TbFUT1* 5'- and

228   3'-UTRs. After selection with puromycin, an ectopic copy of *TbFUT1,* under the control of a

229   tetracycline-inducible promoter, was introduced in the ribosomal DNA (rDNA) locus using

230   phleomycin selection. Following induction with tetracycline, the second allele was replaced with

231   the *BSD* gene by homologous recombination, generating the final procyclic form

232   *ΔTbFUT1::PAC/TbFUT1^{Ti}/ΔTbFUT1::BSD* conditional null mutant cell line (PCF *TbFUT1*

233   cKO). In bloodstream form cells (Fig. 4, middle panel), an ectopic copy of *TbFUT1* carrying a C-

234   terminal MYC$_3$ epitope tag under the control of a tetracycline-inducible promoter was first

235   introduced into the ribosomal DNA (rDNA) locus using phleomycin selection. Following cloning

236   and induction with tetracycline, the first *TbFUT1* allele was then targeted for homologous

237   recombination with linear DNA containing the hygromycin resistance gene (*HYG*) flanked by

238   about 1200 bp of the *TbFUT1* 5'- and 3'-UTRs. After selection with hygromycin, Southern

239   blotting revealed that gene conversion had taken place and that both *TbFUT1* alleles had been

240   replaced   by   *HYG*   yielding   a   bloodstream   form   *TbFUT1*-

241   *MYC$_3$^{Ti}/ΔTbFUT1::HYG/ΔTbFUT1::HYG* conditional null mutant cell line (BSF *TbFUT1*-MYC$_3$

242   cKO). Southern blotting data confirming the genotypes of these mutants are shown in Fig. S7.

243   The BSF cell line was also used to generate a *TbFUT1^{Ti}/ΔTbFUT1::HYG/ΔTbFUT1::HYG*

244   conditional null mutant cell line by *in situ* homologous recombination of the tetracycline

245   inducible *TbFUT1*-MYC$_3$ copy, converting it to an untagged *TbFUT1* gene and generating BSF

246   *TbFUT1* cKO (Fig. 4, right panel).

247

248   ***TbFUT1 is essential to procyclic and bloodstream form T. brucei.*** Procyclic and bloodstream

249   form *TbFUT1* conditional null mutants were grown under permissive (plus tetracycline) or non-

250   permissive (minus tetracycline) conditions. The PCF *TbFUT1* cKO cells grown under non-

251   permissive conditions showed a clear reduction in the rate of cell growth after 6 days, eventually

252   dying after 15 days (Fig. 5*A*). The BSF *TbFUT1* cKO cells grew like wild type cells under

253   permissive conditions, whether or not the expressed TbFUT1 had a C-terminal MYC$_3$ tag, and

254   under non-permissive conditions also showed a clear reduction in the rate of cell growth after 2-4

255   days, dying after 3-5 days (Fig. 5*B* and *C*). These growth phenotypes are very similar to those

256   described for procyclic and bloodstream form *TbGMD* conditional null mutants that cannot

257   synthesise GDP-Fuc under non-permissive conditions (Fig. S8) (26). This is consistent with the

258   hypothesis that TbFUT1 may be the only enzyme that utilizes GDP-Fuc, or at least that it is the

259   only FUT transferring fucose to essential acceptors. Further evidence that TbFUT1 is essential for

260   procyclic and bloodstream form growth was obtained from Northern blots (Fig. 5*D* and *E*). These

261   show that *TbFUT1* mRNA levels are undetectable for several days after the removal of

262   tetracycline, but that growth resumes only when some cells escape tetracycline control after about

263   29 days (procyclic form) and 11 days (bloodstream form). Escape from tetracycline control after

264   several days is typical of conditional null mutants for essential trypanosome genes (18). Evidence

265   for the expression of the MYC$_3$ tagged TbFUT1 protein in the BSF *TbFUT1*-MYC$_3$ cKO cell line

266   and of unmodified TbFUT1 in the BSF *TbFUT1* cKO cell line under permissive conditions is

267   shown in (Fig. 5*F*).

268   From a morphological point of view, both procyclic form *TbGMD* and *TbFUT1*

269   conditional null mutants grown under non-permissive conditions showed an increase in average

270   cell volume, due to increased cell length, concomitant with the start of the cell growth phenotype

271   (Fig. S9*A*). However, we were unable to reproduce the flagellar detachment phenotype previously

272   reported for the PCF *TbGMD* cKO grown in non-permissive conditions (26), nor was such a

273   phenotype observed in the PCF *TbFUT1* cKO parasites, either by scanning electron microscopy

274   or immunofluorescence (Fig. S9*C* and S10). The percentage of cells displaying flagellar

275   detachment (1.5-2 %) in both null mutants grown in non-permissive conditions (Fig. S9*B*) was

276   consistent with what has previously been reported for wild type cells (62). Additionally, we could

277   observe no defect in cell motility in either PCF *TbGMD* or PCF *TbFUT1* cKO grown in non-

278   permissive conditions (Fig. S11).

279

280   ***TbFUT1 localizes to the parasite mitochondrion.*** The BSF *TbFUT1*-MYC$_3$ cKO cell line, grown

281   under permissive conditions, was stained with anti-MYC antibodies and produced a pattern

282   suggestive of mitochondrial localization. This was confirmed by co-localization with

283   MitoTracker^{TM} (Fig. 6*A*). However, when TbFUT1 was introduced into wild type cells fused with

284   an HA$_3$ epitope tag at the N-terminus, either with or without a C-terminal MYC$_3$-tag (constructs

285   pLEW100:HA$_3$-FUT1-MYC$_3$ and pLEW100:HA$_3$-FUT1), the tagged protein co-localized with

286   GRASP, a marker of the Golgi apparatus (Fig. 6*B* and *C*). In these cases, we suspect that N-

287   terminal tagging has disrupted mitochondrial targeting, by obscuring the N-terminal

288   mitochondrial targeting sequence. Indeed, no mitochondrial targeting motif was predicted *in*

289   *silico* for N-terminal HA$_3$ tagged TbFUT1. Nevertheless, since the mitochondrial localization of a

290   fucosyltransferase is unprecedented, we elected to raise polyclonal antibodies against

291   recombinant TbFUT1 to further assess its subcellular location. To do so, an N-terminally His$_6$-

292   tagged Δ_{32}TbFUT1 protein was expressed, re-solubilized from inclusion bodies and used for

293   rabbit immunization. The IgG fraction was isolated on immobilized protein-A and the anti-

294   TbFUT1 IgG sub-fraction affinity purified on immobilized recombinant GST-TbFUT1 fusion

295   protein. To further ensure mono-specificity of the antibodies to TbFUT1, the resulting fraction

296   was adsorbed against a concentrated cell lysate of the PCF *TbFUT1* cKO mutant grown for 9 days

297   under non-permissive conditions. The resulting highly-specific polyclonal antibody was used to

298   detect TbFUT1 expression in wild type bloodstream form cells as well as in BSF and PCF

299   *TbFUT1* cKO cells under permissive and non-permissive conditions (Fig. 7*A-C*). Anti-TbFUT1

300   antibodies co-localized with MitoTracker^{TM} staining in the wild-type cells and in the conditional

301   null mutants under permissive conditions. No signal for the anti-TbFUT1 antibodies was seen

302   under non-permissive conditions, confirming the specificity of the polyclonal antibody. Taking

303   the possibility of a dual Golgi/mitochondrial localization into account, TbFUT1 localization was

304   also assessed in bloodstream form cells ectopically expressing TbGnTI-HA$_3$ as an authentic Golgi

305   marker (63). No co-localization between TbGnTI-HA$_3$ and anti-TbFUT1 was observed,

306   suggesting that TbFUT1 is either exclusively or predominantly expressed in the parasite

307   mitochondrion (Fig. 7*D*).

308

309   ***Deletion of TbFUT1 disturbs mitochondrial activity.*** Bloodstream form wild type and BSF

310   *TbFUT1* cKO cells, grown with and without tetracycline for 5 days, were stained with antibodies

311   to mitochondrial ATPase and with MitoTracker^{TM}. As expected ATPase and MitoTracker^{TM} co-

312   localized in wild type cells and in the mutant under permissive conditions (Fig. 8, top panels).

313   However, under non-permissive conditions the few remaining viable cells showed significantly

14

314   diminished MitoTracker^{TM} staining, indicative of reduced mitochondrial membrane potential, and

315   a reduction in ATPase staining, suggesting that TbFUT1 is in some way required for

316   mitochondrial function (Fig. 8, lower panels, and Fig. S12).

317

318   **DISCUSSION**

319   The presence and essentiality of the nucleotide sugar donor GDP-Fuc in BSF and PCF

320   trypanosomes lead us to search for putative FUTs in the parasite genome. Only one gene

321   (*TbFUT1*; Tb927.9.3600), belonging to the CAZy GT11 family, was found and phylogenetic

322   analyses revealed that one, or two in the case of *T. cruzi*, orthologues could be found in the

323   genomes of other kinetoplastids. These putative kinetoplastid FUTs form a distinct clade within

324   the GT11 FUT superfamily and are distinct from the GT10 FUTs found in *T. cruzi, L. major* and

325   related parasites, which are absent in *T. brucei*. Consistent with TbFUT1 being the only enzyme

326   likely to utilise the essential metabolite GDP-Fuc, we found that TbFUT1 is also essential to both

327   BSF and PCF parasites. We were able to express TbFUT1 in *E. coli* and the recombinant enzyme

328   was used to demonstrate its activity as a GDP-Fuc : βGal α-1,2 fucosyltransferase with a

329   preference for a Galβ1,3GlcNAcβ1-O-R acceptor motif out of the acceptor substrates

330   investigated.

331   The highly unusual result was the localization of TbFUT1 to the parasite mitochondrion,

332   using an affinity-purified antibody raised against native TbFUT1 as well as C-terminal epitope

333   tagging. Although in recent years fucosylation has been described in the nucleus and cytosol of

334   protists and plants (35, 36, 38, 64), we are unaware of any other examples of mitochondrial FUTs

335   in any organism. Mitochondrial glycosylation in general is poorly understood. The only other

336   known example of a mitochondrial-localized glycosyltransferase is mOGT (45). Mitochondria of

337   rat cardiomyocytes are also positive for OGA and express a UDP-GlcNAc transporter on their

338   outer membrane, indicating all of the molecular components required for this cycling post-

339   translational modification are present in the organelle (46). Interestingly, disruption of mOGT in

340   HeLa cell mitochondria also leads to mitochondrial disfunction. While there are no (m)OGT

341   orthologues in kinetoplastids, these observations highlight some of the challenges inherent for a

342   mitochondrial-localized glycosyltransferase. Firstly, for TbFUT1 to be active, GDP-Fuc needs to

343   be imported into the mitochondrion, suggesting the presence of an uncharacterized mitochondrial

344   GDP-sugar transporter. Secondly, TbFUT1 appears to be an α-1,2-FUT that decorates glycans

345   terminating in Galβ1,3GlcNAc, suggesting either that additional uncharacterized

346   glycosyltransferases and nucleotide sugar transporters may be present in the parasite

347   mitochondrion, or that the glycoconjugate substrate is assembled in the secretory pathway and

348   then somehow imported into the mitochondrion to be modified by TbFUT1. Experiments to

349   resolve these options will be undertaken, as will further experiments to try to find the protein,

350   lipid and/or other acceptor substrates of TbFUT1. The latter may then provide clues as to why

351   TbFUT1 is essential for mitochondrial function and parasite growth. Several attempts to identify

352   TbFUT1 substrates have failed so far, these include fucose-specific lectin blotting and pull-

353   downs, [^{3}H]fucose labelling of parasites transfected with GDP-Fuc salvage pathway enzymes and

354   LC-MS/MS precursor ion and neutral-loss scanning methods. Although the significance is

355   unclear, it is interesting to note that procyclic TbFUT1 has been recently shown to be under

356   circadian regulation (65).

357   In conclusion, *Tb*FUT1 is an essential, mitochondrial *α*-1,2-FUT with orthologues

358   throughout the kinetoplastidia. Although no data is available so far on the enzymes from other

359   members of this group, these initial results suggest the intriguing possibility of an essential,

360   conserved mitochondrial fucosylation pathway in kinetoplastids that might be exploitable as a

361   common drug target.

16

362

363   **EXPERIMENTAL PROCEDURES**

364   **Parasite strains.** *T. brucei* procyclic form (strain 427, clone 29.13) and bloodstream form (strain

365   427, variant MITaT 1.2) were used in these experiments. Both strains are stably expressing T7

366   polymerase and tetracycline repressor protein under G418 (bloodstream) or G418 and

367   hygromycin (procyclic) selection (66). Details on media and selection antibiotics can be found in

368   the SI Methods.

369

370   **Cloning, protein expression and purification of TbFUT1.** The putative *TbFUT1*

371   (Tb927.9.3600) was identified via BLASTp searches as described in Methods SI. The open

372   reading frame (ORF) was amplified by PCR from *T. brucei* strain 427 genomic DNA and cloned

373   into the N-terminal GST fusion vector pGEX-6P-1, modified to contain the PreScission Protease

374   site (kind gift of Prof. Daan Van Aalten). The resulting pGEX6P1-GST-PP-*Tb*FUT1 was

375   transformed into BL21 (DE3) *E. coli* strain. Recombinant protein expression was induced with

376   isopropyl-β-D-thiogalactopyranoside (IPTG) and carried out at 16°C for 16 h. GST-TbFUT1 was

377   isolated from the soluble fraction by affinity purification with Glutathione Sepharose Fast Flow

378   beads. Recombinant protein identification by peptide mass fingerprinting was performed by the

379   Proteomic and Mass Spectrometry facility, School of Life Sciences, University of Dundee.

380   Primer sequences and details on cloning, expression, and purification can be found in the SI

381   Methods.

382

383   **Fucosyltransferase activity assays.** Aliquots of 2 μg of affinity purified GST-TbFUT1 were

384   incubated with 1 μCi GDP[^{3}H]Fuc (American Radiochemicals), 1 mM acceptor in 50 mM Tris-

385   HCl, 25 mM KCl, 5 mM $MgCl_2$, 5 mM $MnCl_2$, pH 7.2 for 2 h at 37°C. The acceptors tested

17

386   (Table 1) were purchased from Sigma, Dextra Laboratories or Toronto Research Chemicals. To

387   study the dependency on divalent cations, $MgCl_2$ and $MnCl_2$ were removed from the buffer and a

388   formulation with 10 mM EDTA was also tested. Reactions were stopped by cooling on ice, then

389   desalted on mixed bed columns as detailed in SI Methods. About 5% of the desalted reactions

390   were counted at a LS 6500 scintillation counter (Beckmann). The remaining material was

391   lyophilized for further analyses.

392

393   **HPTLC analysis**. Reaction products and standards were dissolved in 20% 1-propanol and

394   separated on a 10 cm HPTLC Si-60 plates (Merck) using 1-propanol:acetone:water 9:6:4 (v:v:v)

395   as mobile phase. Non-radiolabelled sugars were visualized by orcinol/ H_2SO_4 staining. In the case

396   of radiolabelled products, the HPTLC plates were sprayed with En[3]hance[®] (PerkinElmer) and

397   visualized by fluorography.

398

399   **Large scale TbFUT1 assay and product purification.** Acceptor (5 mM Lacto-N-biose-β-O-

400   methyl) and donor (2.5 mM GDP-Fuc) were incubated with 8 μg affinity purified GST-TbFUT1

401   in 20 mM Tris-HCl, 25 mM KCl, pH 7.2 at 37°C for 24 h. The reaction products were desalted on

402   a mixed-bed column and lyophilized. The trisaccharide product was isolated by normal phase

403   liquid chromatography on an amino column as described in Methods SI. The fractions containing

404   the putative trisaccharide product were pooled and lyophilized.

405

406   **Permethylation, ESI-MS analysis and GC-MC methylation linkage analysis.** Purified

407   TbFUT1 reaction product was dried and permethylated by the sodium hydroxide method as

408   described in (68). Aliquots were used for ESI-MS and the remainder was subjected to acid

409   hydrolysis followed by NaB^2H_4 reduction and acetylation (67). The resulting PMAAs were

410   analysed using an HP6890 GC System equipped with an HP-5 column linked to a 5975C mass

411   spectrometer (Agilent). For ESI-MS and ESI-MS/MS, the permethylated glycans were directly

412   infused into a Q-Star XL mass spectrometer equipped with Analyst software (Applied

413   Biosystems). See Methods SI for details.

414

415   **NMR.** The purified TbFUT1 reaction product was exchanged in ^{2}H$_2$O by freeze-drying and

416   analysed by one-dimensional ^{1}H-NMR and two-dimensional ^{1}H-ROESY (Rotating frame

417   Overhouser Effect SpectroscopY). All spectra were acquired on a Bruker Avance spectrometer

418   operating at 500 MHz with a probe temperature of 293°K.

419

420   **Generation of *TbFUT1* conditional null mutants.** About 500 bp of the 5' and 3' untranslated

421   regions (UTRs) immediately flanking the *TbFUT1* ORF were amplified from *T. brucei* genomic

422   DNA (gDNA) and linked together by PCR. Antibiotic resistance cassettes were cloned into the

423   *Hind*III/*BamH*I restriction sites between the two UTRs to generate constructs either containing

424   puromycin acetyltransferase (*PAC*) or blastacidin S deamidase (*BSD*). In addition, a hygromycin

425   (HYG) based *TbFUT1* gene replacement cassette was generated with longer UTRs (1.25 kb). The

426   tetracycline-inducible ectopic copy construct was generated by amplifying the *TbFUT1* ORF

427   from *T. brucei* gDNA and cloning the resulting PCR product into pLEW100. Additionally, a

428   modified pLEW100 vector was generated which allowed universal tagging of a protein of interest

429   with a C-terminal 3x MYC tag. Linearized DNA was used to transform the parasites as

430   previously described (66, 68, 69). The genotype of the transformed parasites was verified by

431   Southern blot. For details see Methods SI.

432

19

433   **Northern blotting**. Total RNA was prepared from $5x10^6$-$1x10^7$ cells using the RNeasy MIDI Kit

434   (Qiagen) according to manufacturer's instructions. The RNA was separated on a 2% agarose-

435   formaldehyde gel, blotted and detected using the Northern Starter Kit (Roche). Probes were

436   designed based on the DIG RNA Labelling Kit T7 (Roche) and *TbFUT1* and alpha-tubulin

437   (Tb427.01.2340) templates were amplified from *T. brucei* bloodstream form gDNA using primers

438   P17/P18 and P19/P20 (Table S2), respectively. Total RNA and DIG labelled probes were quality

439   checked by capillary electrophoresis on an Agilent BioAnalyzer 2100.

440

441   **Generation and expression of epitope-tagged TbFUT1 constructs.** *TbFUT1* was introduced in

442   two different sites of pLEW100HXM (see Methods SI) to yield HA_3-TbFUT1 and HA_3-TbFUT1-

443   MYC_3. TbFUT1 was amplified using primers P21/P22 for HA_3-TbFUT1 and P23/P16 for HA_3-

444   TbFUT1-MYC_3 (Table S2). The two plasmids were purified and electroporated into BSF cells as

445   described above. The generation of the TbFUT1-MYC_3 cell line is described above as it was used

446   to generate the BSF *TbFUT1* cKO cell line.

447

448   **Preparation of anti-FUT1 antibody**. An N-terminally truncated construct encoding Δ_{32}TbFUT1

449   fused to an N-terminal hexahistidine tag (HIS_6) with PreScission plus (PP) protease cleavage site

450   in a pET15b expression vector was introduced into BL21 (DE3) gold *E.coli* cells. *E. coli* cells

451   were allowed to express His_6-PP-TbFUT1 over night at 25°C in auto-inducing media (5052-NPS-

452     $MgSO_4$). The recombinant HIS_6-PP-Δ_{32}TbFUT1 protein was resolubilized from inclusion bodies

453   as described in Methods SI. Re-solubilised protein (2 mg) was sent off to DC Biosciences [LTD] for

454   production of polyclonal rabbit antiserum. See Methods SI for details on the purification of the

455   anti-TbFUT1 IgG fraction.

456

20

457   **Immunofluorescence microscopy.** Late log phase *T. brucei* bloodstream form or procyclic cells

458   were fixed in 4% PFA/PBS in solution. When using Mitotracker^{TM} Red CMX Ros cell cultures

459   were spiked with a 25 nM concentration over 20 minutes, before harvesting. Permeabilization,

460   blocking and labelling conditions are described in Methods SI. Microscopy was performed on a

461   DeltaVision Spectris microscope (GE Healthcare) and images were processed using Softworx.

462

463   **ACKNOWLEDGEMENTS**

472

REFERENCES

1. Matthews KR (2005) The developmental cell biology of *Trypanosoma brucei*. *J Cell Sci* 118(Pt 2):283–290.

2. Cross GAM (1996) Antigenic variation in trypanosomes: Secrets surface slowly. *Bioessays* 18(4):283–291.

3. Pays E (1998) Expression and function of surface proteins in *Trypanosoma brucei*. *Mol Biochem Parasitol* 91(1):3–36.

4. Mehlert A, Richardson JM, Ferguson MA (1998) Structure of the glycosylphosphatidylinositol membrane anchor glycan of a class-2 variant surface glycoprotein from *Trypanosoma brucei*. *J Mol Biol* 277(2):379–392.

5. Schwede A, Carrington M (2010) Bloodstream form trypanosome plasma membrane proteins: antigenic variation and invariant antigens. *Parasitology* 137(14):2029–2039.

6. Richardson JP, Beecroft RP, Tolson DL, Liu MK, Pearson TW (1988) Procyclin: an unusual immunodominant glycoprotein surface antigen from the procyclic stage of African trypanosomes. *Mol Biochem Parasitol* 31(3):203–216.

7. Treumann A, et al. (1997) Structural characterisation of two forms of procyclic acidic repetitive protein expressed by procyclic forms of *Trypanosoma brucei*. *J Mol Biol* 269(4):529–547.

8. Roditi I, Furger A, Ruepp S, Schürch N, Bütikofer P (1998) Unravelling the procyclin coat of *Trypanosoma brucei*. *Mol Biochem Parasitol* 91(1):117–130.

9. Vassella E, et al. (2001) Multiple procyclin isoforms are expressed differentially during the development of insect forms of *Trypanosoma brucei*. *J Mol Biol* 312(4):597–607.

10. Vassella E, Bütikofer P, Engstler M, Jelk J, Roditi I (2003) Procyclin null mutants of *Trypanosoma brucei* express free glycosylphosphatidylinositols on their surface. *Mol Biol Cell* 14(4):1308–1318.

11. Roper JR (2005) The Suppression of Galactose Metabolism in Procyclic Form *Trypanosoma*

499   *brucei* Causes Cessation of Cell Growth and Alters Procyclin Glycoprotein Structure and

500   Copy Number. *J Biol Chem* 280(20):19728–19736.

501 12. Nagamune K, et al. (2004) Surface Sialic Acids Taken from the Host Allow Trypanosome

502   Survival in Tsetse Fly Vectors. *J Exp Med* 199(10):1445–1450.

503 13. Güther MLS, et al. (2009) Fate of glycosylphosphatidylinositol (GPI)-less procyclin and

504   characterization of sialylated non-GPI-anchored surface coat molecules of procyclic-form

505   *Trypanosoma brucei*. *Eukaryot Cell* 8(9):1407–1417.

506 14. Nagamune K, et al. (2000) Critical roles of glycosylphosphatidylinositol for *Trypanosoma*

507   *brucei*. *Proc Natl Acad Sci USA* 97(19):10336–10341.

508 15. Chang T, Milne KG, Güther MLS, Smith TK, Ferguson MAJ (2002) Cloning of

509   *Trypanosoma brucei* and *Leishmania major* genes encoding the GlcNAc-

510   phosphatidylinositol de-N-acetylase of glycosylphosphatidylinositol biosynthesis that is

511   essential to the African sleeping sickness parasite. *J Biol Chem* 277(51):50176–50182.

512 16. Smith TK, Crossman A, Brimacombe JS, Ferguson MAJ (2004) Chemical validation of GPI

513   biosynthesis as a drug target against African sleeping sickness. *EMBO J* 23(23):4701–4708.

514 17. Urbaniak MD, Crossman A, Ferguson MAJ (2008) Probing *Trypanosoma brucei*

515   Glycosylphosphatidylinositol Biosynthesis Using Novel Precursor-Analogues. *Chem Biol*

516   *Drug Des* 72(2):127–132.

517 18. Roper JR, Guther MLS, Milne KG, Ferguson MAJ (2002) Galactose metabolism is essential

518   for the African sleeping sickness parasite *Trypanosoma brucei*. *Proc Natl Acad Sci USA*

519   99(9):5884–5889.

520 19. Urbaniak MD, Turnock DC, Ferguson MAJ (2006) Galactose starvation in a bloodstream

521   form *Trypanosoma brucei* UDP-glucose 4'-epimerase conditional null mutant. *Eukaryot*

522   *Cell* 5(11):1906–1913.

523 20. Urbaniak MD, et al. (2006) Identification of novel inhibitors of UDP-Glc 4′-epimerase, a

524   validated drug target for african sleeping sickness. *Bioorg Med Chem Lett* 16(22):5744–

525   5747.

526   21.   Stokes MJ, et al. (2008) The Synthesis of UDP-N-acetylglucosamine Is Essential for
527   Bloodstream Form *Trypanosoma brucei* in Vitro and in Vivo and UDP-N-acetylglucosamine
528   Starvation Reveals a Hierarchy in Parasite Protein Glycosylation. *J Biol Chem*
529   283(23):16147–16161.

530   22.   Denton H, Fyffe S, Smith TK (2010) GDP-mannose pyrophosphorylase is essential in the
531   bloodstream form of *Trypanosoma brucei*. *Biochem J* 425(3):603–614.

532   23.   Marino K, et al. (2011) Characterization, Localization, Essentiality, and High-Resolution
533   Crystal Structure of Glucosamine 6-Phosphate N-Acetyltransferase from *Trypanosoma*
534   *brucei*. *Eukaryot Cell* 10(7):985–997.

535   24.   Marino K, et al. (2010) Identification, subcellular localization, biochemical properties, and
536   high-resolution crystal structure of *Trypanosoma brucei* UDP-glucose pyrophosphorylase.
537   *Glycobiology* 20(12):1619–1630.

538   25.   Turnock DC, Ferguson MAJ (2007) Sugar nucleotide pools of *Trypanosoma brucei,*
539   *Trypanosoma cruzi*, and *Leishmania major*. *Eukaryot Cell* 6(8):1450–1463.

540   26.   Turnock DC, Izquierdo L, Ferguson MAJ (2007) The de novo synthesis of GDP-fucose is
541   essential for flagellar adhesion and cell growth in *Trypanosoma brucei*. *J Biol Chem*
542   282(39):28853–28863.

543   27.   Guo H, et al. (2017) Genetic metabolic complementation establishes a requirement for GDP-
544   fucose in *Leishmania*. *J Biol Chem* 292(25):10696–10708.

545   28.   Cooper R, de Jesus AR, Cross GA (1993) Deletion of an immunodominant *Trypanosoma*
546   *cruzi* surface glycoprotein disrupts flagellum-cell adhesion. *J Cell Biol* 122(1):149–156.

547   29.   Haynes PA, Ferguson MA, Cross GA (1996) Structural characterization of novel
548   oligosaccharides of cell-surface glycoproteins of *Trypanosoma cruzi*. *Glycobiology*
549   6(8):869–878.

550   30.   Allen S, Richardson JM, Mehlert A, Ferguson MAJ (2013) Structure of a complex
551   phosphoglycan epitope from gp72 of *Trypanosoma cruzi*. *J Biol Chem* 288(16):11093–
552   11105.

553   31.   Coutinho PM, Deleury E, Davies GJ, Henrissat B (2003) An Evolving Hierarchical Family
554   Classification for Glycosyltransferases. *J Mol Biol* 328(2):307–317.

555   32.   Lombard V, Golaconda Ramulu H, Drula E, Coutinho PM, Henrissat B (2013) The
556   carbohydrate-active enzymes database (CAZy) in 2013. *Nucleic Acids Res* 42(D1):D490–
557   D495.

558   33.   Martinez-Duncker I (2003) A new superfamily of protein-*O*-fucosyltransferases, 2-
559   fucosyltransferases, and 6-fucosyltransferases: phylogeny and identification of conserved
560   peptide motifs. *Glycobiology* 13(12):1C–5.

561   34.   Breton C, Oriol R, Imberty A (1998) Conserved structural features in eukaryotic and
562   prokaryotic fucosyltransferases. *Glycobiology* 8(1):87–94.

563   35.   Rahman K, et al. (2016) The E3 Ubiquitin Ligase Adaptor Protein Skp1 Is Glycosylated by
564   an Evolutionarily Conserved Pathway That Regulates Protist Growth and Development. *J
565   Biol Chem* 291(9):4268–4280.

566   36.   Van Der Wel H, Fisher SZ, West CM (2002) A bifunctional diglycosyltransferase forms the
567   Fucalpha1,2Galbeta1,3-disaccharide on Skp1 in the cytoplasm of *Dictyostelium*. *J Biol
568   Chem* 277(48):46527–46534.

569   37.   West CM, Wang ZA, Van Der Wel H (2010) A cytoplasmic prolyl hydroxylation and
570   glycosylation pathway modifies Skp1 and regulates O2-dependent development in
571   *Dictyostelium*. *Biochim Biophys Acta* 1800(2):160–171.

572   38.   Zentella R, et al. (2017) The *Arabidopsis O*-fucosyltransferase SPINDLY activates nuclear
573   growth repressor DELLA. *Nat Chem Biol* 161:1279.

574   39.   Gas-Pascual E, et al. (2019) CRISPR/Cas9 and glycomics tools for *Toxoplasma*
575   glycobiology. *J Biol Chem* 294(4):1104–1125.

576   40.   Priest JW, Hajduk SL (1994) Developmental regulation of mitochondrial biogenesis in
577   *Trypanosoma brucei*. *J Bioenerg Biomembr* 26(2):179–191.

578   41.   Jensen RE, Englund PT (2012) Network news: the replication of kinetoplast DNA. *Annu

579   *Rev Microbiol* 66:473–491.

580   42. Povelones ML (2014) Beyond replication: Division and segregation of mitochondrial DNA
581   in kinetoplastids. *Mol Biochem Parasitol* 196(1):53–60.

582   43. Ogbadoyi EO, Robinson DR, Gull K (2003) A high-order trans-membrane structural linkage
583   is responsible for mitochondrial genome positioning and segregation by flagellar basal
584   bodies in trypanosomes. *Mol Biol Cell* 14(5):1769–1779.

585   44. Kung LA, et al. (2009) Global analysis of the glycoproteome in *Saccharomyces cerevisiae*
586   reveals new roles for protein glycosylation in eukaryotes. *Mol Syst Biol* 5:308.

587   45. Bond MR, Hanover JA (2015) A little sugar goes a long way: the cell biology of *O*-GlcNAc.
588   *J Cell Biol* 208(7):869–880.

589   46. Banerjee PS, Ma J, Hart GW (2015) Diabetes-associated dysregulation of *O*-GlcNAcylation
590   in rat cardiac mitochondria. *Proc Natl Acad Sci U S A* 112(19):6050–6055.

591   47. Sacoman JL, Dagda RY, Burnham-Marusich AR, Dagda RK, Berninsone PM (2017)
592   Mitochondrial *O*-GlcNAc Transferase (mOGT) Regulates Mitochondrial Structure,
593   Function, and Survival in HeLa Cells. *J Biol Chem* 292(11):4499–4518.

594   48. Zhang L, et al. (2010) *Helicobacter hepaticus* Hh0072 gene encodes a novel 1-3-
595   fucosyltransferase belonging to CAZy GT11 family. *Glycobiology* 20(9):1077–1088.

596   49. Wang G, Boulton PG, Chan NW, Palcic MM, Taylor DE (1999) Novel *Helicobacter pylori*
597   alpha1,2-fucosyltransferase, a key enzyme in the synthesis of Lewis antigens. *Microbiology*
598   145 (Pt 11)(11):3245–3253.

599   50. Kelly RJ, Rouquier S, Giorgi D, Lennon GG, Lowe JB (1995) Sequence and expression of a
600   candidate for the human Secretor blood group alpha(1,2)fucosyltransferase gene (FUT2).
601   Homozygosity for an enzyme-inactivating nonsense mutation commonly correlates with the
602   non-secretor phenotype. *J Biol Chem* 270(9):4640–4649.

603   51. Li M, et al. (2008) Characterization of a Novel α1,2-Fucosyltransferase of *Escherichia coli*
604   O128:B12 and Functional Investigation of Its Common Motif. *Biochemistry* 47(1):378–387.

605   52. Takahashi T, et al. (2000) A sequence motif involved in the donor substrate binding by alpha1,6-fucosyltransferase: the role of the conserved arginine residues. *Glycobiology* 10(5):503–510.

608   53. Horton P, Nakai K (1997) Better prediction of protein cellular localization sites with the k nearest neighbors classifier. *Proc Int Conf Intell Syst Mol Biol* 5:147–152.

610   54. Emanuelsson O, Nielsen H, Brunak S, von Heijne G (2000) Predicting Subcellular Localization of Proteins Based on their N-terminal Amino Acid Sequence. *J Mol Biol* 300(4):1005–1016.

613   55. Claros MG, Vincens P (1996) Computational method to predict mitochondrially imported proteins and their targeting sequences. *Eur J Biochem* 241(3):779–786.

615   56. Krnáčová K, Vesteg M, Hampl V, Vlček Č, Horváth A (2012) Euglena gracilis and Trypanosomatids possess common patterns in predicted mitochondrial targeting presequences. *J Mol Evol* 75(3-4):119–129.

618   57. Long S, Jirku M, Ayala FJ, Lukes J (2008) Mitochondrial localization of human frataxin is necessary but processing is not for rescuing frataxin deficiency in *Trypanosoma brucei*. *Proc Natl Acad Sci U S A* 105(36):13468–13473.

621   58. Aslett M, et al. (2009) TriTrypDB: a functional genomic resource for the Trypanosomatidae. *Nucleic Acids Res* 38(suppl_1):D457–D462.

623   59. Beyer TA, Hill RL (1980) Enzymatic-Properties of the Beta-Galactoside-Alpha-1-] 2 Fucosyl-Transferase From Porcine Sub-Maxillary Gland. *J Biol Chem* 255(11):5373–5379.

625   60. Kamińska J, Wiśniewska A, Kościelak J (2003) Chemical modifications of α1,6-fucosyltransferase define amino acid residues of catalytic importance. *Biochimie* 85(3-4):303–310.

628   61. Pettit N, et al. (2010) Characterization of WbiQ: An α1,2-fucosyltransferase from *Escherichia coli* O127:K63(B8), and synthesis of H-type 3 blood group antigen. *Biochem Biophys Res Commun* 402(2):190–195.

631   62. LaCount DJ, Barrett B, Donelson JE (2002) *Trypanosoma brucei* FLA1 Is Required for
632   Flagellum Attachment and Cytokinesis. *J Biol Chem* 277(20):17580–17588.

633   63. Damerow M, et al. (2014) Identification and Functional Characterization of a Highly
634   Divergent *N*-Acetylglucosaminyltransferase I (TbGnTI) in *Trypanosoma brucei*. *J Biol*
635   *Chem* 289(13):9328–9339.

636   64. Bandini G, et al. (2016) *O*-fucosylated glycoproteins form assemblies in close proximity to
637   the nuclear pore complexes of *Toxoplasma gondii*. *Proc Natl Acad Sci USA* 113(41):11567–
638   11572.

639   65. Rijo-Ferreira F, Pinto-Neves D, Barbosa-Morais NL, Takahashi JS, Figueiredo LM (2017)
640   *Trypanosoma brucei* metabolism is under circadian control. *Nature Microbiol* 2:17032.

641   66. Wirtz E, Leal S, Ochatt C, Cross GA (1999) A tightly regulated inducible expression system
642   for conditional gene knock-outs and dominant-negative genetics in *Trypanosoma brucei*.
643   *Mol Biochem Parasitol* 99(1):89–101.

644   67. Ferguson MAJ (1992) Chemical and enzymatic analysis of glycosylphosphoditylinositol
645   anchors. *Lipid Modification of Proteins: A Practical Approach* (IRL Press, Oxford), pp 191–
646   230.

647   68. Burkard G, Fragoso CM, Roditi I (2007) Highly efficient stable transformation of
648   bloodstream forms of *Trypanosoma brucei. Mol Biochem Parasitol* 153(2):220–223.

649   69. Güther MLS, Lee S, Tetley L, Acosta-Serrano A, Ferguson MAJ (2006) GPI-anchored
650   proteins and free GPI glycolipids of procyclic form *Trypanosoma brucei* are nonessential for
651   growth, are required for colonization of the tsetse fly, and are not the only components of the
652   surface coat. *Mol Biol Cell* 17(12):5265–5274.

653

654

655   Table 1. Acceptor substrates and semi-quantitative fucosyltransferase activities.

*Tb*FUT1 Activity	Lane of Fig. 1	Abbreviat.	Name	Structure
+++	2, 5, 8	LNB	lacto-N-biose	**Galβ1,3GlcNAc**
+++	23	LNB-OMe	lacto-N-biose-O-methyl	**Galβ1,3GlcNAc**β-OMe
++	13	LNT	lacto-N-tetraose	**Galβ1,3GlcNAc**β1,3Galβ1,4Glc
++	16	LNH	lacto-N-hexaose	**Galβ1,3GlcNAc**β1,3(Galβ1,4GlacNAcβ1,6)Galβ1,4Glc
++	1	Lac	lactose	Galβ1,4Glc
+	15	iLNO	iso-lacto-N-octaose	**Galβ1,3GlcNAc**β1,3(**Galβ1,3GlacNAc**β1,3Galβ1,4GlcNAcβ1,6)Galβ1,4Glc
+	3	LacNAc	N-acetyllactosamine	Galβ1,4GlcNAcN
+	12	LNnH	lacto-N-neohexaose	Galβ1,4GlcNAcβ1,3(Galβ1,4GlcNAcβ1,6)Galβ1,4Glc
+	14	LNnT	lacto-N-neotetraose	Galβ1,4GlcNAcβ1,3Galβ1,4Glc
+	18	3'-FL	3'-fucosyllactose	Galβ1,4(Fucα1,3)Glc
-	11	β-Gal	β-galactose	β-Gal
-	17	GNG	β1,6-galactosyl-N-acetyl-glucosamine	Galβ1,6GlcNAc
-	19	1,6GB	β1,6-galactobiose	Galβ1,6Gal
-	20	1,4GB	galabiose	Galα1,4Gal
-	21	LB2TS	Linear B2 trisaccharide	Galα1,3Galβ1,4GlcNAc
-	22	β-Gal-OMe	β-galactose-O-methyl	β-Gal-OMe
-	24	2'-FL	2'-fucosyllactose	Fucα1,2Galβ1,4Glc

656   [a] The relative efficiencies of the acceptors to act as substrates (+++, ++, + and -) are based on visual

657   inspection of the intensities of the products bands in Figure 1.

658

659   Table 2. PMAAs derivatives identified by GC-MS methylation linkage analysis of the purified

660   TbFUT1 reaction product.

PMAA derivative	RT (min)	Origin
4,6-di-*O*-methyl-1,3,5-Tri-*O*-acetyl-(1-^{2}H)- 2-N-methylacetamidoglucosaminitol	24.6	3-*O*-substituted GlcNAc
2,3,4,6-tetra-*O*-methyl-1,5-di-*O*-acetyl-(1-^{2}H)-galactitol	16.7	Non-reducing terminal Gal
3,4,6-tri-*O*-methyl-1,2,5-tri-*O*-acetyl-(1-^{2}H)-galactitol	18.6	2-*O*-substituted Gal
2,3,4-tri-*O*-methyl-1,5-di-*O*-acetyl-(1-^{2}H)-fucositol	14.1	Non-reducing terminal Fuc
3,4-di-*O*-methyl-1,2,5-tri-*O*-acetyl-(1-^{2}H)-fucositol	15.9	2-*O*-substituted Fuc

661   RT: retention time
662

30

663 Table 3. ^{1}H and ^{1}H ROESY chemical shift assignments for the purified TbFUT1 reaction product.
664

Residue	H_1	H_2	H_3	H_4	H_5	$H_{6/6'}$	NAc
αFuc	5.05 (J=4 Hz)	3.57	3.67	3.63	4.2	1.1	
βGal	4.5	3.45	3.55	3.89	ND	ND	
βGlcNAc	ND	3.63	ND	3.4	ND	3.78/3.89	2.1

665
666
667 J: coupling
668 ND: chemical shift could not be clearly assigned
669
670

31

FIGURE LEGENDS
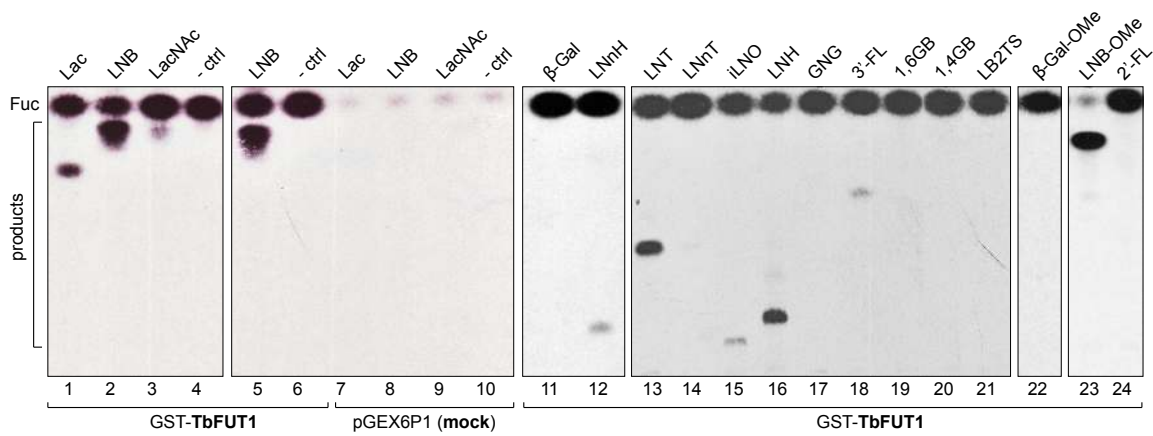
FIGURE 1. **Recombinant GST-TbFUT1 transfers [^{3}H]Fuc to a variety of sugar acceptors.**
Each assay used 2 μg of purified GST-TbFUT1, GDP-[^{3}H]Fuc and 1 mM of acceptor. Reaction products were desalted and separated by silica HPTLC, and detected by fluorography. The acceptor abbreviations above each lane are defined in Table 1. - *ctrl*: negative control reaction missing the acceptor.

32

679
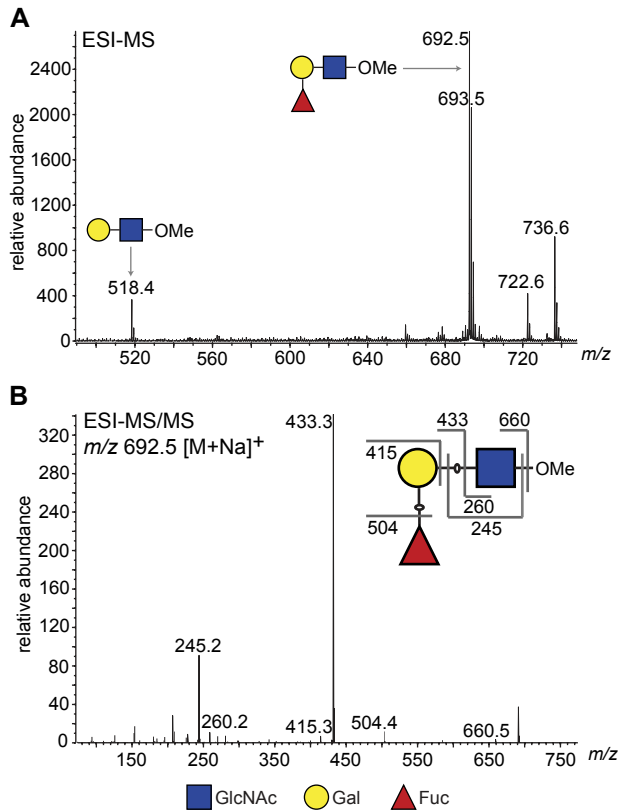
FIGURE 2. **ESI-MS and ESI-MS/MS of TbFUT1 *in vitro* reaction product**. *A*. ESI-MS of the purified and permethylated reaction product. The ion at *m/z* 692.5 is consistent with the [M + Na]$^+$ ion of a permethylated trisaccharide of composition $dHex_1Hex_1HexNAc_1$. Some of the unmodified acceptor ($Hex_1HexNAc_1$) could still be observed (*m/z* 518.4). *B*. MS/MS product ion spectrum of *m/z* 692.5. The collision-induced fragmentation pattern indicated that the dHex (Fuc) residue was linked to the Hex (Gal) and not to the HexNAc (GlcNAc) residue.

686
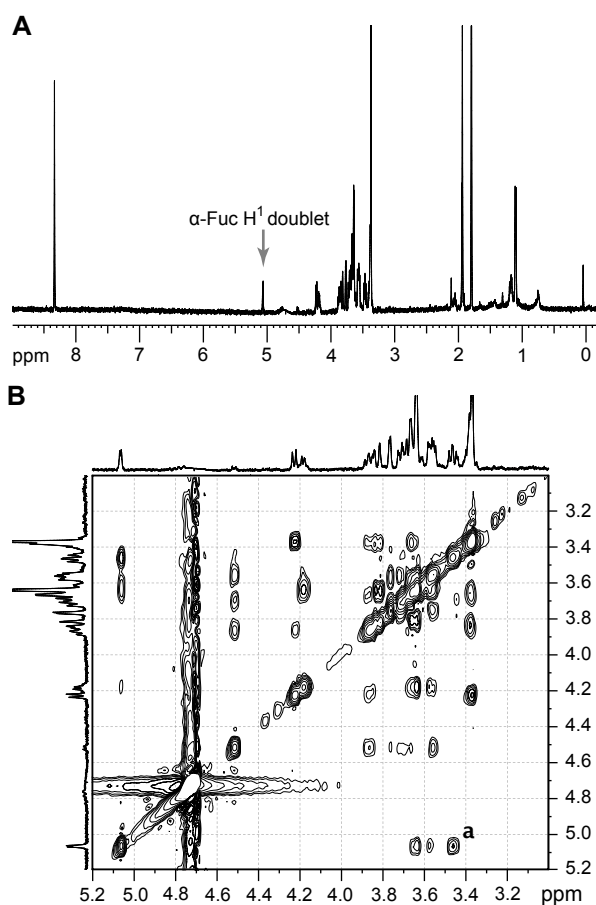
FIGURE 3. **^{1}H NMR and ^{1}H ROESY spectra of the TbFUT1 reaction product.** *A*. One-dimensional ^{1}H-NMR spectrum. The *arrow* points to the α-Fuc H_1 doublet. *B*. Enlargement of the 3.2-5.1 ppm region of the two-dimensional ^{1}H ROESY. *a* indicates the signal for a crosspeak resulting from a through-space connectivity between α-Fuc H_1 and β-Gal H_2.
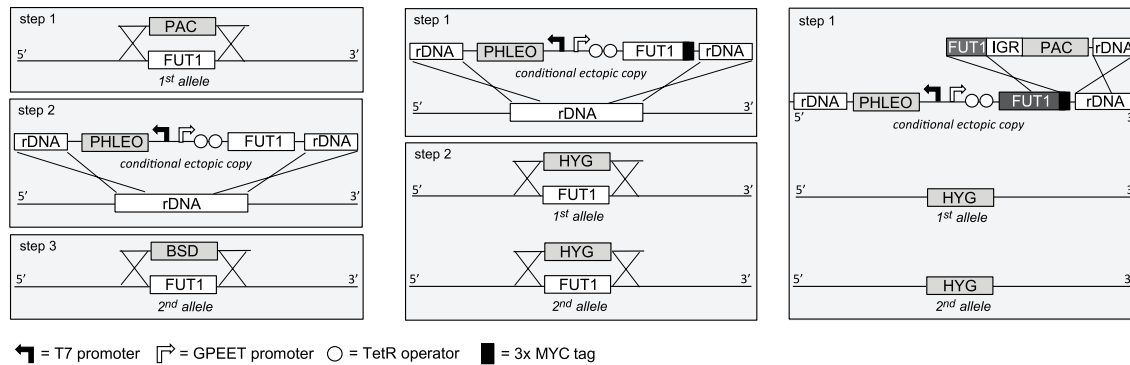
FIGURE 4. **Cloning strategies for the creation of the *TbFUT1* conditional null mutants**. *Left panel*: To create the procyclic form conditional null mutant (PCF *TbFUT1* cKO) the first *TbFUT1* allele was replaced by *PAC*, an ectopic tetracycline-inducible copy of the *TbFUT1* gene was introduced into the ribosomal DNA locus and the second *TbFUT1* allele was replaced by *BSD*. *Middle panel*: To create the bloodstream form conditional null mutant (BSF *TbFUT1-MYC₃* cKO) an ectopic tetracycline-inducible copy of the *TbFUT1* gene with a MYC$_3$ tag was first introduced into the ribosomal DNA locus. Both *TbFUT1* alleles were subsequently replaced by *HYG* through homologous recombination followed by gene conversion. *Right panel:* To create the untagged bloodstream form cKO (BSF *TbFUT1* cKO), the BSF *TbFUT1-MYC₃* cKO mutant (*middle panel*) was modified by homologous recombination with a construct that removed the C-terminal MYC$_3$ tag under *PAC* selection.
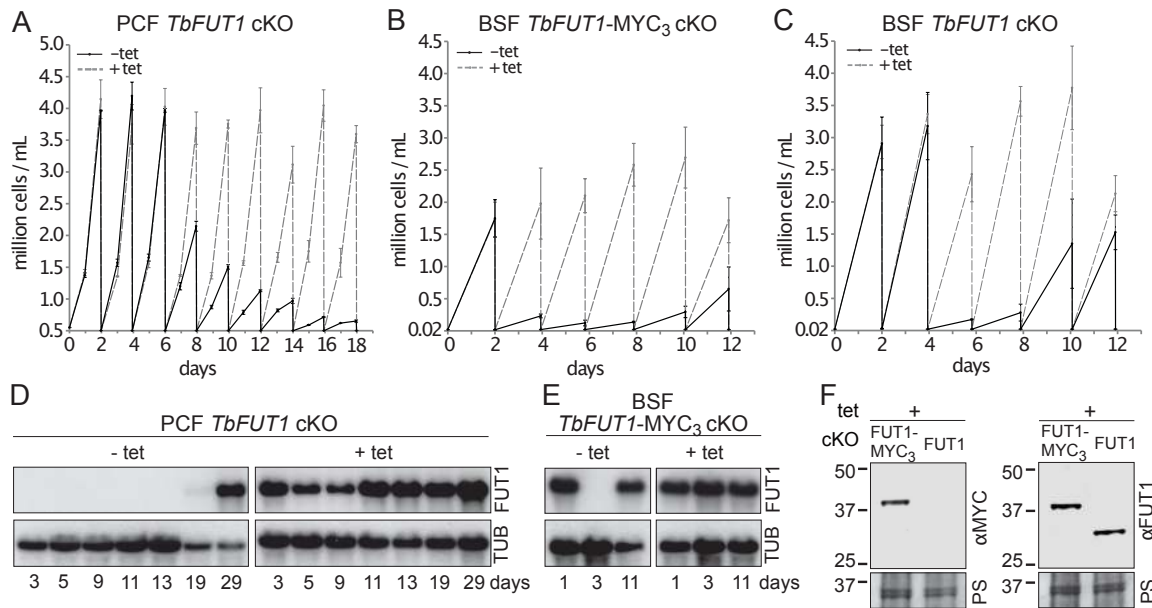
FIGURE 5. **TbFUT1 is essential for procyclic and bloodstream form cell growth *in vitro*.** The cell numbers (± standard deviation) for TbFUT1 cKO under permissive (plus tetracycline, *dotted line*) and non-permissive (minus tetracycline, *solid line*) conditions are shown for three procyclic (*A*) and bloodstream form (*C*) clones, as well as for three bloodstream clones carrying a tetracycline-inducible ectopic *TbFUT1* gene with a C-terminal MYC_3 tag (*B*). *D-E*. Corresponding *TbFUT1* mRNA levels were determined by Northern blots. Alpha-Tubulin (TUB) was used as a loading control. *F*. TbFUT1-MYC_3 and untagged TbFUT1 are detected by Western blot analysis in the respective bloodstream form cKO cell lines under permissing conditions (+ Tet). The *left panel* shows an anti-MYC (αMYC) blot and the *right panel* an anti-recombinant TbFUT1 antibody (αFUT1) blot. Membranes were stained with Ponceau S (PS) to ensure equal loading.
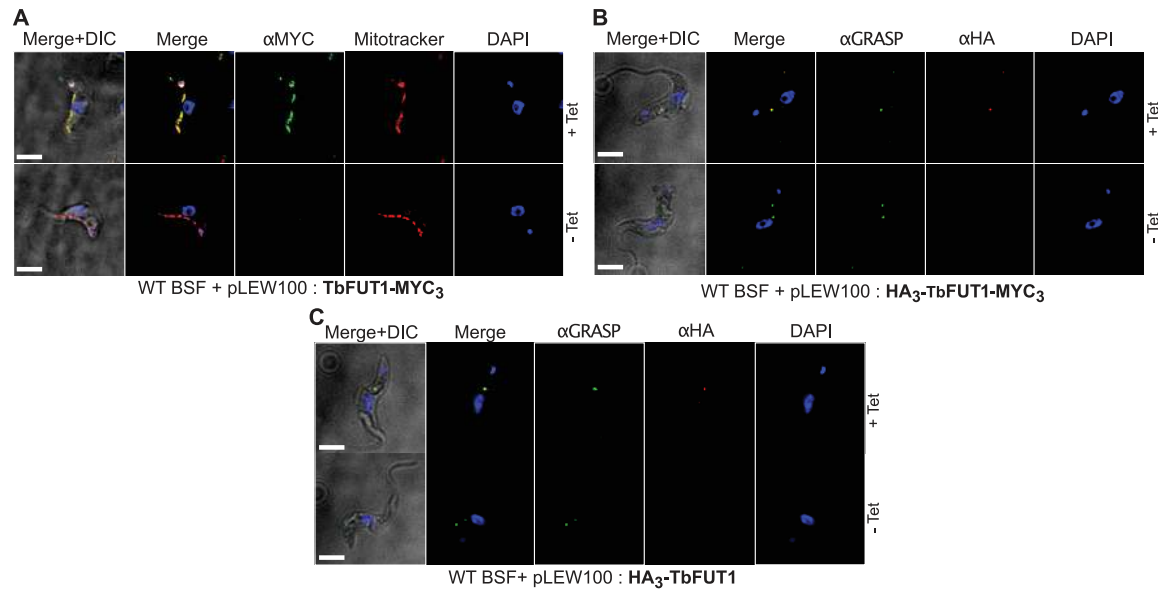
719

FIGURE 6. **The C- and N-terminal tagging of TbFUT1 result in mitochondrial and Golgi apparatus localization, respectively**. *A.* Bloodstream form (BSF) cKO parasites expressing tet-inducible C-terminally tagged TbFUT1-MYC$_3$ were imaged under permissive (+Tet) and non-permissive (-Tet) conditions by DIC and fluorescence microscopy after staining with anti-MYC, MitoTracker^{TM}, and DAPI. Comparable patterns were observed for anti-MYC and MitoTracker^{TM}, suggesting TbFUT1-MYC$_3$ localizes to the mitochondrion. *B-C.* IFA of BSF cKO parasites expressing a tet-inducible N-terminally tagged HA$_3$-TbFUT1-MYC$_3$ (*B*) or HA$_3$-TbFUT1 (*C*) after labelling with anti-HA, anti-GRASP, and DAPI suggests a Golgi apparatus location for both HA$_3$-TbFUT1-MYC$_3$ and HA$_3$-TbFUT1. The absence of anti-MYC (*A*) or anti-HA (*B-C*) staining under non-permissive conditions confirms the specificity of the labelling for the respective TbFUT1 fusion proteins. Scale bars: 3 μm.

731

37
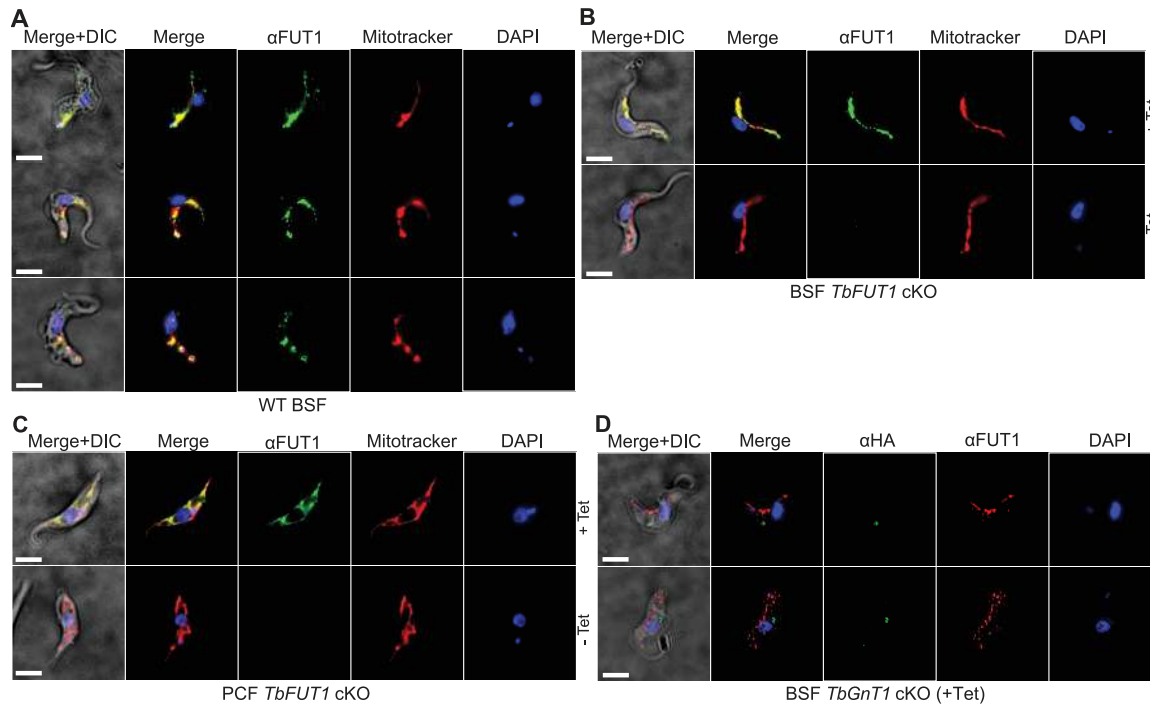
FIGURE 7. **Antibodies to the recombinant protein localize TbFUT1 to the mitochondrion**. *A.* IFA of wild type bloodstream form (BSF) trypanosomes after staining with affinity purified anti-TbFUT1 (αFUT1) MitoTracker^{TM} and DAPI. Comparable patterns were observed for anti-TbFUT1 and MitoTracker^{TM}, suggesting TbFUT1 localizes to the mitochondrion. *B-C.* Bloodstream (*B*) and procyclic (*C*) form *TbFUT1* conditional null mutants were imaged under permissive (+Tet) and non-permissive (-Tet) conditions. In both cases the tetracycline-inducible TbFUT1 pattern is consistent with a mitochondrial localization. *D.* BSF trypanosomes induced to express a C-terminally tagged known Golgi glycosyltransferase (TbGnTI-HA$_3$) were imaged after staining with αFUT1, anti-HA and DAPI, as indicated. The merged images of two representative cells suggest no significant co-localization between native TbFUT1 and the Golgi-localized TbGnT1. Scale bars: 3 μm.

745
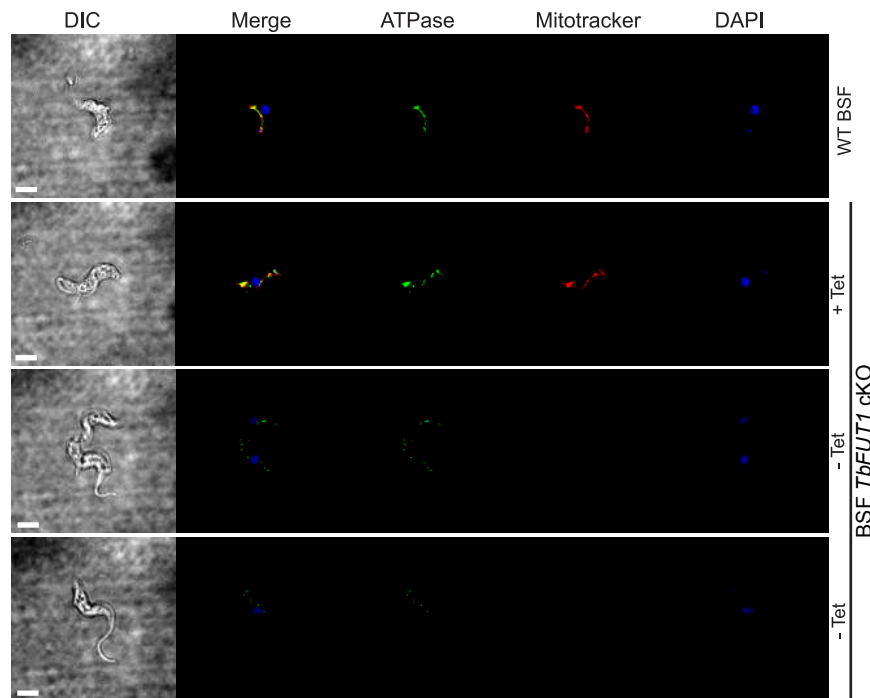
FIGURE 8. **Absence of TbFUT1 disturbs mitochondrial activity.** Bloodstream form (BSF) wild type and *TbFUT1* cKO parasites were cultured for 5 days under permissive (+ Tet) and non-permissive (- Tet) conditions, fixed and labelled with Mitotracker™ for mitochondrial potential and with anti mitichondrial-ATPase antibody. In mutants grown in non-permissive conditions (*lower panels*) both ATPase and Mitotracker staining are strongly reduced, suggesting reduced mitochondrial functionality. Scale bar: 3 μm.

752